arXiv:cond-mat/0607816v2 [cond-mat.str-el] 15 Dec 2006

Electronic properties of correlated metals in the vicinity of a charge order transition: optical spectroscopy of α-(BEDT-TTF)$_2M$Hg(SCN)$_4$ (M = NH$_4$, Rb, Tl)

N. Drichko[1,2], M. Dressel[1], C. A. Kuntscher[1] *, A. Pashkin[1],* A. Greco[3], J. Merino[4], and J. Schlueter[5]
[1] *1. Physikalisches Institut, Universität Stuttgart, Pfaffenwaldring 57, 70550 Stuttgart, Germany*
[2] *Ioffe Physico-Technical Institute, St.Petersburg, Russia*
[3] *Facultad de Ciencias Exactas Ingeniería y Agrimensura e Instituto de Física Rosario (UNR-CONICET), Rosario, Argentina*
[4] *Dept. de Fisica Teorica de la Materia Condensada, Universidad Autonoma de Madrid, Spain*
[5] *Material Science Division, Argonne National Laboratory, Argonne, Illinois 60439-4831, U.S.A.*
(Dated: February 6, 2008)

The infrared spectra of the quasi-two-dimensional organic conductors α-(BEDT-TTF)$_2$-MHg(SCN)$_4$ (M = NH$_4$, Rb, Tl) were measured in the range from 50 to 7000 cm^{-1} down to low temperatures in order to explore the influence of electronic correlations in quarter-filled metals. The interpretation of electronic spectra was confirmed by measurements of pressure dependent reflectance of α-(BEDT-TTF)$_2$KHg(SCN)$_4$ at T=300 K. The signatures of charge order fluctuations become more pronounced when going from the NH$_4$ salt to Rb and further to Tl compounds. On reducing the temperature, the metallic character of the optical response in the NH$_4$ and Rb salts increases, and the effective mass diminishes. For the Tl compound, clear signatures of charge order are found albeit the metallic properties still dominate. From the temperature dependence of the electronic scattering rate the crossover temperature is estimated below which the coherent charge-carriers response sets in. The observations are in excellent agreement with recent theoretical predictions for a quarter-filled metallic system close to charge order.

PACS numbers: 71.10.Hf, 71.30.+h, 74.25.Gz, 74.70.Kn

I. INTRODUCTION

Electron-electron interactions are well recognized to be decisive for the ground states observed in low-dimensional electronic systems, for instance Mott insulator, charge-ordered state, superconductivity, ferro- and antiferromagnetic order. The generic phase diagram of correlated materials shows a number of important features: the variation of crucial (order) parameters like the electron doping or the effective electronic interactions drives the system from a metal to an ordered state, with superconductivity found around some critical point.[1,2] While in the high-temperature superconductors the control parameter typically is the hole doping, the quasi-two dimensional-organic conductors give a possibility to nicely tune the effective electronic interactions.[3] The well-developed phase diagram of half-filled BEDT-TTF-based organic conductors demonstrates this approach: the ground state of systems changes from a metal (Fermi liquid) to a Mott insulator on the increase of electronic correlations, with superconductivity found in between.[4,5]

Besides the on-site Coulomb interaction U, for the quarter-filled systems the nearest-neighbor electronic repulsion V is the second important parameter. In the case of large values of U, a change of the ground state from metallic to a charge-ordered on the increase of V was proposed for the quarter-filled layered molecular conductors; around the quantum critical point superconductivity mediated by charge fluctuations was suggested.[6] The family of quarter-filled organic conductors α-(BEDT-TTF)$_2M$Hg(SCN)$_4$ (M=NH$_4$, Rb, Tl, K) is a prime candidate to experimentally study the vicinity of a phase border between metallic and charge ordered states in the phase diagram calculated in Ref. 6 and schematically shown in Fig. 8 of this work: the NH$_4$ compound exhibits superconductivity at $T_c \approx 1$ K, while the others are metallic with a density-wave state observed below 10 K, which is still subject to discussion.[7,8] In the present investigation we are interested in the temperature region above the density wave state where the band structure and Fermi surface of these isostructural compound are basically identical.

These crystals are composed by alternating layers of two types: conductivity occurs in layers of BEDT-TTF [bis-(ethylenedithio)tetrathiafulvalene] molecules, while the layers of the polymeric anions $[M\mathrm{Hg(SCN)_4}]^-$ serve as a 'charge reservoir'; in the following we refer to the various salts by their metal ions M=NH$_4$, Rb, Tl, or K in the anion layer. They have the same valence but different volume, which effects the size of the unit cell and hence the transfer integrals t between the BEDT-TTF molecules in the conducting layer in some non-trivial way,[9] leading to a different V/t parameter between the compounds.

A change of the control parameter V/t by chemical modifications in the anionic layer was extensively utilized by H. Mori *et al.*[10] when synthesizing the quarter-filled family θ-(BEDT-TTF)$_2MM'$(SCN)$_4$. These quarter-filled compounds are closer to an insulating charge order state, and the transition temperature between the metallic and insulating phase decreases as the ratio V/t shrinks. A phase diagram was proposed based on resistivity studies which exhibits the general features as mentioned above.[1,6] A number of experiments prove that the charge disproportionation already develops in the metallic phase at temperatures well above the phase transition.[11,12] In θ-(BEDT-TTF)$_2$RbZn(SCN)$_4$, for ex-

ample, the width of the lines observed in NMR experiments suggests a slowly fluctuating charge order.[11] On the other hand, the only charge-order insulator of the α-phase family, α-(BEDT-TTF)$_2$I$_3$,[13,14] exhibits a timely stable charge disproportionation[15] already at temperatures above the insulating state.

While those investigations lowered the temperature in order to move towards the metal-insulator transition, a particulary interesting possibility would be to tune the V/t ratio to approach the phase transition to the insulating state from the metallic side. Do charge-order fluctuations develop? Or do stable regions form which are partly charge ordered? Is this a first order or a second order phase transition? Will charge-order fluctuations be enhanced although the system remains metallic? The α-(BEDT-TTF)$_2M$Hg(SCN)$_4$ family is the proper system to address these questions.

Optical investigations in a wide frequency range are most suitable to characterize the charge dynamics and to identify deviation from a simple metallic behavior.[16,17,18] For quarter-filled systems close to charge order, the frequency-dependent conductivity was calculated by exact diagonalization for large U and different V/t ratios.[19] The spectral weight is expected to shift from the Drude peak to higher frequencies as correlations intensify. It is further proposed that the effective mass of the charge carriers and their scattering rate depends on correlations and temperature[19]. In previous optical studies clear signatures of charge-order fluctuations have been observed in α-(BEDT-TTF)$_2$KHg(SCN)$_4$ in contrast to the superconducting analog α-(BEDT-TTF)$_2$NH$_4$KHg(SCN)$_4$.[20] It is now of great interest to extend our investigations to the whole family of α-(BEDT-TTF)$_2M$Hg(SCN)$_4$ materials and to compare the experimental findings with the theory. This gives us insight on how quarter-filled two-dimensional metallic system behave close to a correlation-driven charge-order transition.

The paper is structured in the following way, in Section II we present the experimental techniques, in Section III we present the results, a primary analysis of the observed spectra (B) and its interpretation (C), and in (D) we show that pressure-dependent measurements confirm our interpretation, in E and F we discuss the nature of the major anisotropy and temperature-dependent effects. In Section IV we further interpret our results in terms of metallic quarter-filled system close to charge order and an ordered system. Our findings are summarized in Section V (conclusions.)

II. EXPERIMENTAL TECHNIQUES

Single crystals of α-(BEDT-TTF)$_2M$Hg(SCN)$_4$ (M=NH$_4$, Rb, Tl) were grown according to Ref. 21 and reach up to 2×2 mm^2 in the highly conducting ac-plane; the crystal structure was confirmed by X-ray diffraction. When characterized by dc resistivity, the results coincide with previous reports. The polarized reflectivity of the crystals was measured in the conducting plane along the main optical axes, parallel and perpendicular to the stacks of BEDT-TTF molecules (i.e. parallel c and a crystal axes) in the frequency range between 50 and 7000 cm^{-1}. The main axes were identified at room temperature by polarization dependence measurements with an accuracy of 2°. The spectral resolution used was 1 cm^{-1} for the NH$_4$ and Tl salts and 2 cm^{-1} in the case of α-(BEDT-TTF)$_2$RbHg(SCN)$_4$. The sample was cooled in a cold-finger cryostat with a rate of circa 1 K/min; spectra were taken at 300, 200, 150, 100, 50 and 6 K. In order to receive the absolute values of reflectivity, the sample covered *in situ* with 100 nm gold was used as a reference; this technique is described in Ref. 22. Although these measurements agree with previously published spectra[20,23,24] as far as the overall shape is concerned, the absolute values are up to 5% higher due to our superior method of measuring the absolute reflectivity value. The mid-infrared data were also double checked at room temperature using an infrared microscope with a spot size of 100 μm. We were not able to use this improved technique for the low-temperature measurements of α-(BEDT-TTF)$_2$KHg(SCN)$_4$ due to poor quality and small size of the crystals; thus we do not extend the present quantitative analysis of the optical data to this compound.

The optical conductivity was evaluated by the Kramers-Kronig analysis of the reflection spectra. The spectra in the 9000-40000 cm^{-1} were measured at room temperature using a home-made microspectroreflectometer; at frequencies above 40000 cm^{-1} the common ω^{-2} and ω^{-4} extrapolations were used, while a Hagen-Rubens assumption was applied at low frequencies. The agreement obtained with the dc conductivity is excellent. In the case of the NH$_4$ salt, for instance, the measured dc values range from $\sigma_{\rm dc} = 100$ to 400 $(\Omega{\rm cm})^{-1}$ at ambient temperature and 100 times higher at $T = 4.2$ K; the value for optical conductivity at $\omega \to 0$ is about 350 $(\Omega{\rm cm})^{-1}$ at 300 K and 36000 $(\Omega{\rm cm})^{-1}$ at $T = 6$ K.

Polarized reflectance measurements of α-(BEDT-TTF)$_2$KHg(SCN)$_4$ under pressure were performed using a diamond anvil cell equipped with type IIA diamonds suitable for infrared measurements. Finely ground CsI powder was chosen as quasi-hydrostatic pressure medium. For the pressure experiment a small piece (about 80 μm $\times$ 100 μm in size) was cut from a single crystal and placed in the hole of a steel gasket. A ruby chip was added for determining the pressure by the ruby luminescence method.[25] The pressure-dependent reflectance was studied in the mid-infrared frequency range ($550 - 8000$ cm^{-1}) at room temperature using a Bruker IFS 66v/S FT-IR spectrometer in combination with an infrared microscope (Bruker IRscope II). Reflectance spectra were measured at the interface between sample and diamond anvil (the measurement geometry is illustrated in Ref. 26); spectra taken at the inner diamond-air interface of the empty cell served as the reference for normalization of the sample spectra. The pressure-

dependent reflectivity spectra reported below refer to the absolute reflectivity at the sample-diamond interface, calculated according to $R_{s-d}(\omega) = R_{\rm dia} \times I_s(\omega)/I_d(\omega)$, where $I_s(\omega)$ denotes the intensity spectrum reflected from the sample-diamond interface and $I_d(\omega)$ the reference spectrum of the diamond-air interface. $R_{\rm dia}$ was calculated from the refractive index of diamond $n_{\rm dia}$ to 0.167. For quantitative description of the spectra, a Drude-Lorentz fit was performed. To get reliable fit parameters, we simultaneously fitted the zero-pressure reflectivity spectra taken inside the cell (with an diamond-sample interface) and the spectra taken outside the cell with an air-sample interface. The change of the parameters of the Drude part and the Lorentz oscillators were then followed as a function of pressure.

III. RESULTS AND ANALYSIS

A. Experimental results

In Figs. 1 to 3 the optical reflectivity and conductivity of the three compounds α-(BEDT-TTF)$_2M$Hg(SCN)$_4$ (M=NH$_4$, Rb, Tl) are displayed. Results for the K-analog have already been presented in Ref. 20. The reflectivity of all the compounds shows a metal-like frequency and temperature behavior: a plasma edge is observed in the mid-infrared, and the high reflectance at frequencies below the plasma edge increases even further upon cooling. The higher reflectivity and conductivity observed in the polarization $E \perp$ stacks is in agreement with the calculated anisotropy of the transfer integrals.[9] The room-temperature spectra of the Rb and Tl salts differ only by few percent, while the NH$_4$ compound shows a slightly higher reflectivity at low frequencies.

A number of vibrational features in the 400 – 1600 cm^{-1} frequency range are known to originate from the coupling of totally symmetric A$_g$ vibrations of BEDT-TTF with electrons (emv coupling).[27] These comparatively weak emv-coupled features evidence for the broken symmetry (dimerization) in the stacks, in agreement with the X-ray structural data. The most prominent of the emv-coupled features is the band of $\nu_4(A_g)$ vibration, which appears as a wide maximum between approximately 1200 and 1400 cm^{-1}. This feature is the same in all the salts, while the lower frequency features show some differences between the compounds, which will be discussed later in this paper. The charge-transfer within the dimers, which activates the totally-symmetric vibrations, is expected in the mid-infrared region, but its intensity might be low, in agreement with the weak vibrational features in comparison to the κ-phases, for example.[28,29,30] The narrow band at about 2100 cm^{-1} is the infrared-active C-N stretching vibration of the SCN groups in the anion layer.

At temperatures below 200 K the slightly different levels and shapes of the far-infrared reflectance observed for the NH$_4$, Rb and Tl salts lead to distinct differences in the conductivity spectra. The low-temperature reflectivity of the NH$_4$ salt is close to 100% in the low-frequency limit but abruptly drops above 700 cm^{-1}, especially apparent in the $E \parallel$ stack polarization. This behavior converts to an intense and extremely narrow zero-frequency peak in the conductivity spectrum; in addition there are two wide bands at approximately 1000 cm^{-1} and 2500 cm^{-1}. Accordingly, the lower reflectivity level and gentler slope obtained for the Rb salt causes a less pronounced and wider zero-frequency peak and more spectral weight in the high-frequency features. The reflectivity of the Tl salt also approaches 100%, but in a more gradual fashion; a bump at about 1000 cm^{-1} is superimposed on the high reflectance background at low temperatures. Accordingly, in the conductivity spectra the Drude-peak is not extremely narrow, and the 1000 cm^{-1} maximum is more pronounced than in the spectra of the other two salts. This tendency is even enhanced in the spectra of α-(BEDT-TTF)$_2$KHg(SCN)$_4$, as described in Ref. 20.

B. Drude-Lorentz analysis

We use a Drude-Lorentz fit to disentangle different contributions to the spectra; simultaneous fits of the reflectivity and conductivity spectra put additional restrictions on the parameters. An insert in Fig. 1(d) is an example of the fit, showing the main electronic features in the conductivity spectra of α-(BEDT-TTF)$_2$NH$_4$Hg(SCN)$_4$ at T = 300 and 6 K. The zero-frequency peak is approximated by a simple Drude contribution; the maximum around 1000 cm^{-1} and the wide band in the mid-infrared range are fitted by a Lorentzian each, yielding the central frequencies ω_t of 1000 and 2500 cm^{-1}, respectively. Only when the Drude-like feature sharpens below 200 K, the 1000 cm^{-1} contribution turns into a real peak. The assessment of the Drude plasma frequency by zero-crossing of ϵ_1[16] in agreement with the fit, however, clearly reveals that it is already present at $T = 300$ K; in contrast to the case of half-filled BEDT-TTF-based compounds where it develops only for $T < 50$ K.[29,30]

The simple Drude formula does not describe perfectly the shape of the zero-frequency conductivity peak, but gives reliable values of the scattering rate (as a half-width of the peak). Since our measurements go down to only 50 cm^{-1}, and the zero-frequency conductivity peak becomes very narrow at low temperatures, we did not carry out an extended Drude analysis,[16] to avoid an over-interpretation of the data.

For the further discussion it is important to consider the redistribution of the spectral weight between these spectral features. For the electronic bands at 1000 and 2500 cm^{-1}, the spectral weight is obtained from the respective Lorentz fit. Since the Drude behavior does not perfectly describe the zero-frequency peak in the optical conductivity (especially for the Rb salt), we deter-

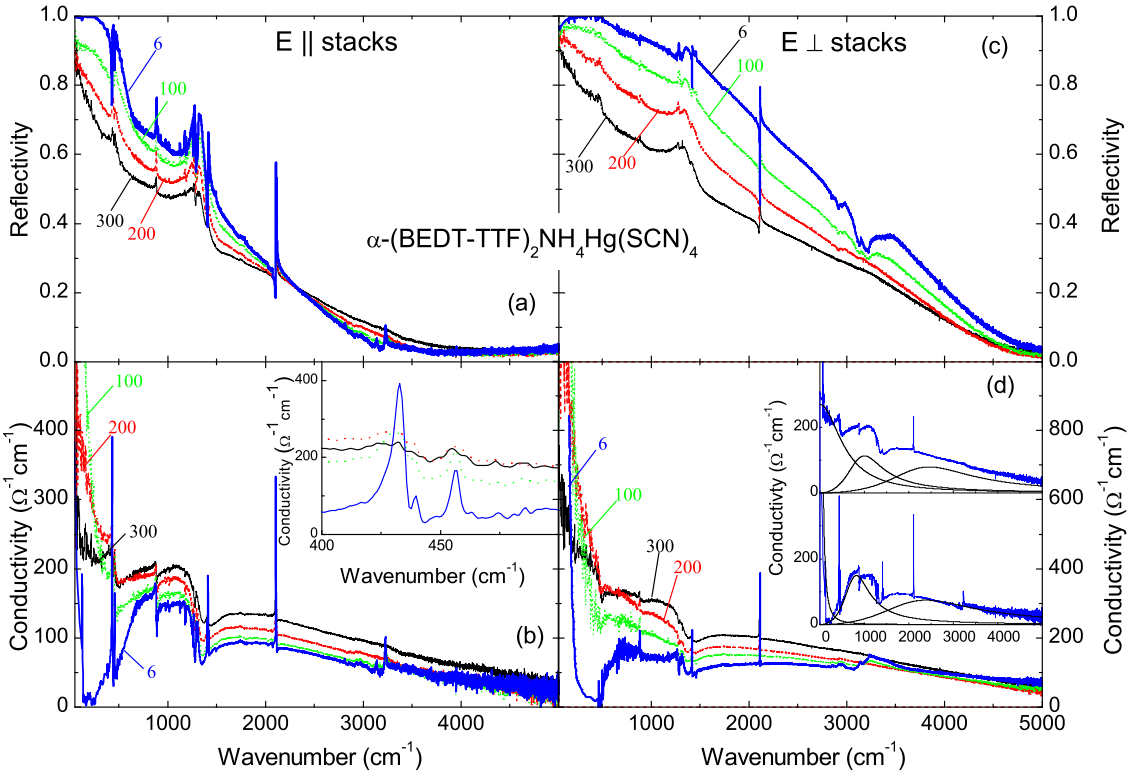

FIG. 1: Color online. Reflectivity and conductivity spectra of α-(BEDT-TTF)$_2$NH$_4$Hg(SCN)$_4$ at T = 300, 200, 100 and 6 K; left panels (a) and (b): $E \parallel$ stacks, right panels (c) and (d): $E \perp$ stacks. The inserts show optical conductivity in the range of $\nu_{12}(A_g)$ and $\nu_{13}(A_g)$ modes. The insert in (d) shows the contributions of one Drude and two Lorentz components for $E \parallel$ stacks 300 K and 6 K.

mined the respective spectral weight by subtracting the two Lorentz oscillators from the experimental spectra.

The spectral weight is received by integration of the optical spectra[16]

$$\omega_p^2 = 8 \int_0^{\omega_c} \sigma_1(\omega)\, \mathrm{d}\omega \quad ; \tag{1}$$

the choice of the upper limit ω_c determines which excitations are considered. The used cut-off (ω_c) value of 7000 cm^{-1} is typical for compounds with similar parameters[29] because is lies well above the plasma edge. According to $\omega_p = (4\pi N e^2/m_b)^{1/2}$, where N is a number of charge carriers known from structural data[21], the spectral weight then yields the band mass m_b. From the spectral weight of the Drude-like contribution $\left(\omega_p^{\mathrm{Drude}}\right)^2$ (see insert (d) in Fig. 1) we can estimate the effective mass of the quasi-free charge carriers m^*. In the following analysis we normally use an effective mass of the charge carriers with respect to the band mass, i.e. the ratio m^*/m_b. The advantage of this approach is that then the effective mass value is normalized according to the thermal contraction of the unit cell.

Within the one dimensional tight-binding approximation, the spectral weight is related to the width of the bands or the transfer integral t:

$$\omega_p^2 = \frac{16 t d^2 e^2}{\hbar^2 V_m} \sin\left\{\frac{\pi}{2}\rho\right\} \quad ; \tag{2}$$

where d is the inter-molecular distance, V_m denotes the volume per molecule, and the number of electrons per site is given by ρ. The enlargement of the spectral weight is related to the increase of the transfer integral; for instance when the temperature decreases and thus the crystal contracts.[31] It is commonly believed[16,29,32] that the total spectral weight is conserved, when the integration in Eq. (1) is extended to high enough values (above 10 000 cm^{-1}). This is not strictly correct[33] when the thermal expansion is extremely large, as in the case of organic materials where it can be as large as 10 %[34], or when external pressure is applied.

C. Assignment of the electronic spectrum

At first we want to make an assignment of the major spectral features which are common to the studied BEDT-TTF salts. The overdamped maximum around 2500 cm^{-1} is observed in the spectra of BEDT-TTF-based organic conductors with different band structures;[29] however, the previously suggested[23]

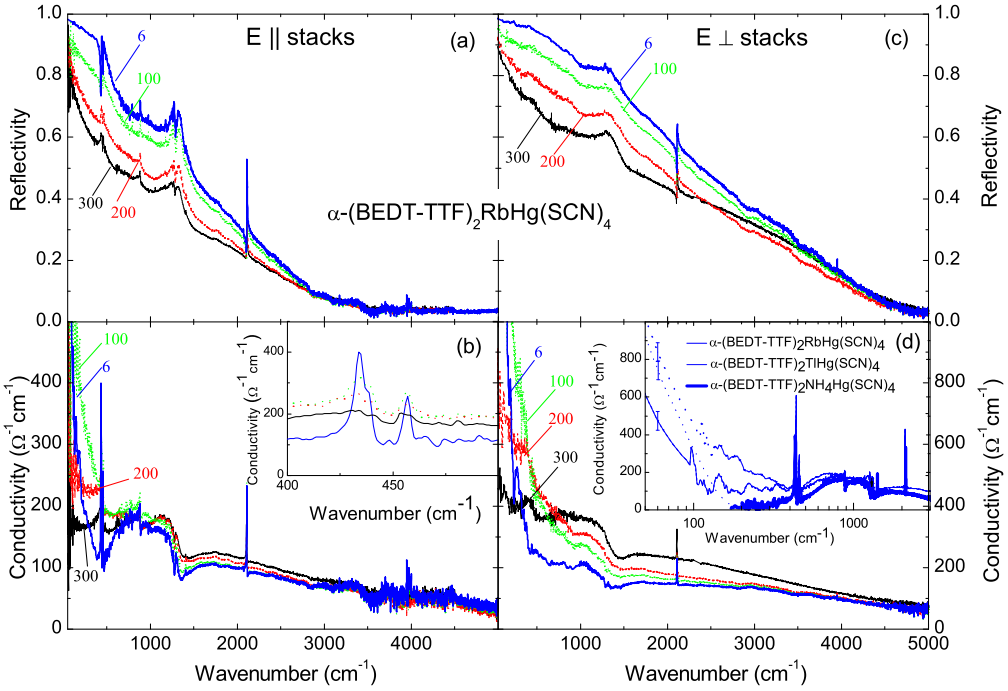

FIG. 2: Color online. Reflectivity and conductivity spectra of α-(BEDT-TTF)$_2$RbHg(SCN)$_4$ at T = 300, 200, 100 and 6 K; left frames (a) and (b): $E \perp$ stacks, right frames (c) and (d): $E \parallel$ stacks. The insert on (b) show optical conductivity in the range of $\nu_{12}(A_g)$ and $\nu_{13}(A_g)$ modes. The insert in (d) present the optical conductivity of the three salts in $E \parallel$ stacks at 6 K in log scale. The low-frequency part presented in dashed lines was received after smoothing the reflectivity data, a respective error bar at 60 cm^{-1} is shown.

assignment to the interband transition is doubtful. Instead we follow the interpretation[35] of the maxima at 1000 cm^{-1} and 2500 cm^{-1} to the spectral weight which is shifted from a zero-peak to higher frequencies due to influence of electronic correlations.[19]

The calculations of Merino *et al.*[19] for metallic quarter-filled systems close to charge order suggest the appearance of two maxima in addition to a Drude peak: a sharper one at $\hbar\omega = 2t$ due to short-range charge order, and a wider one at about $5t$ due to a shift of the spectral weight to high frequencies on the strong influence of correlations. In a very good agreement with the experiment, it gives values of 960 and 2500 cm^{-1} for positions of these features, estimated using t = 0.06 eV, a typical value of transfer integral for these compounds. At room temperature in the polarizations parallel and perpendicular to the stacks the intensity of the two maxima scales with the plasma frequency of the Drude-like contribution, being approximately 1.3 times higher for $E \perp$ stacks; at low temperatures a redistribution of the spectral weight occurs. This encourages the application of the one-band approximation, used by theory, for the analysis of our data: i.e. all features originate from one band modulated by electronic correlations.

Interestingly to note, that while the redistribution of the spectral weight between the features on temperature decrease (which we discuss later) differs between the compounds, the frequencies of the electronic bands exhibit a similar temperature dependence. The low-frequency maximum occurs at the same position in both polarizations and moves down from 1000 cm^{-1} to 800 cm^{-1} when the crystals are cooled to T = 6 K. The changes in the position of the higher-frequency maximum are too small compared to its width and cannot be analyzed.

In order to further prove our interpretation of the electronic spectra let us follow their change upon reducing the V/t ratio.[19] The effective inter-site interaction V/t can be tuned by external pressure: if the distances between the molecules decrease, then the overlap integrals will increase. In fact, the V value will increase as well, but the simple consideration shows that Coloumb repulsion between electrons on the neighboring sites V will increase slower, as $1/d$ (where d is a distance between the molecules), while t will increase exponentially. Alternatively the same effect is achieved by thermal contraction of the crystal, even if accompanied by other temperature-dependent effects. The transfer integrals t of α-(BEDT-TTF)$_2$KHg(SCN)$_4$ calculated for the application of hy-

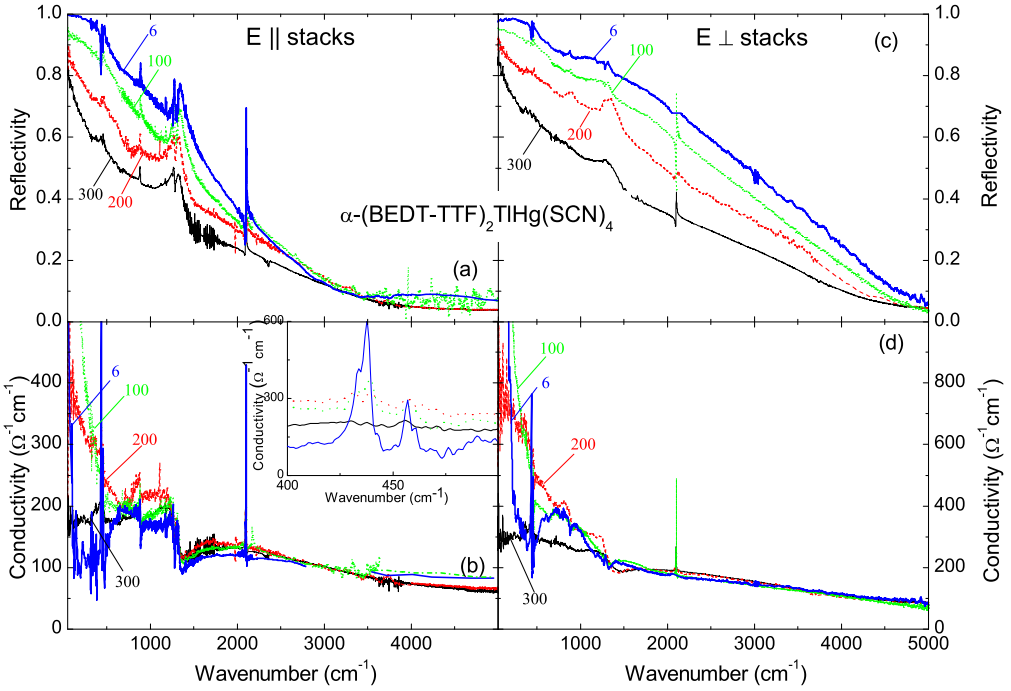

FIG. 3: Color online. Reflectivity and conductivity spectra of α-(BEDT-TTF)$_2$TlHg(SCN)$_4$ at T = 300, 200, 100 and 6 K; panels (a) and (b): $E \perp$ stacks, panels (c) and (d): $E \parallel$ stacks. The inserts show optical conductivity in the range of $\nu_{12}(A_g)$ and $\nu_{13}(A_g)$ modes.

drostatic pressure up to 10 kbar,[36] as well as those for the K, NH_4 and Rb salts calculated from the X-ray data for a wide temperature range[31] show the same tendency. Only one of the intra-stack transfer integrals is expected to increase on cooling[31], while the inter-stack transfer integrals increase by up to 10% on cooling down to 4 K and up to 25% on the application of pressure up to 10 kbar.

D. Pressure dependence of electronic spectra

To support our assignment of electronic spectra of the α-(BEDT-TTF)$_2M$Hg(SCN)$_4$ compounds we performed reflectivity measurements of α-(BEDT-TTF)$_2$KHg(SCN)$_4$ under hydrostatic pressure at room temperature in the 600-7000 cm^{-1} range. The application of the hydrostatic pressure modifies the V/t parameter without changing the temperature-dependent parameters, e.g. scattering rate. Fig. 4 shows, that the main tendency in the spectra on the increasing pressure up to 9.5 kbar is an increase of reflectivity, for lower frequency region in $E \parallel$ stacks direction, and in a wider frequency range for $E\perp$ stacks. The spectral weight of the features estimated by a Drude-Lorentz fit as proposed in Sec. II, illustrates the main tendency (inserts in Fig. 4): the Drude spectral weight increases on the expense of the 1000 and 2500 cm^{-1} maxima. Since the measurements are done in a comparatively narrow spectral range, we cannot comment on a change of the total spectral weight. The reflectivity increase is more pronounced in $E\perp$ stacks direction, but in general the changes are not so anisotropic as was suggested by the transfer integrals calculations.[36]

The shift of the spectral weight from the high-frequency features to the Drude-part is expected since the correlations to bandwidth ratio decreases on rising the transfer integrals: the correlation effects diminish and the systems becomes more metallic. This observation strongly supports our conclusion that the mid-infrared features in the spectra are due to electronic effects. A change of dimerization is not predicted by the calculations;[36] in agreement with this no changes are observed in the BEDT-TTF vibrational features.

E. Temperature dependence of electronic spectra

Upon cooling, the electronic properties of these systems are changed in several respects: (i) As for any metal, the charge-carrier scattering rate is reduced since

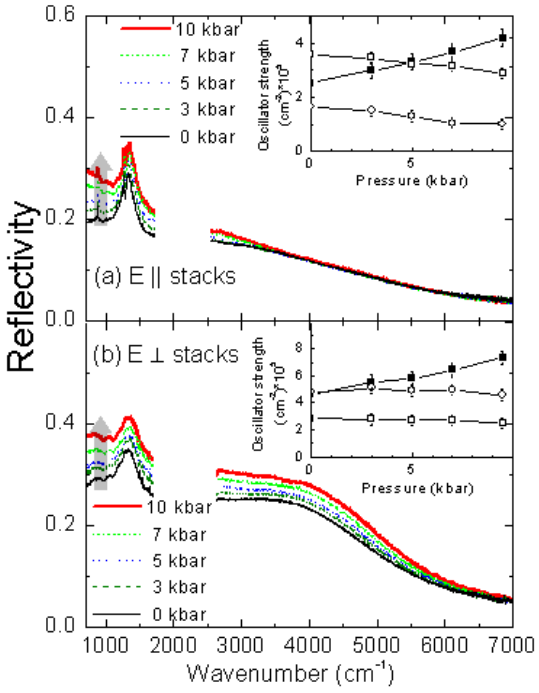

FIG. 4: Color online. Reflectivity and conductivity spectra of α-(BEDT-TTF)$_2$KHg(SCN)$_4$ at 0, 3, 5, 7 and 10 kbar. left panels (a) and (b): $E \parallel$ stacks, right panels (c) and (d): $E \perp$ stacks. The spectral region between 1700 and 2500 cm^{-1}is cut out from the spectra since it is affected by the strong absorbance of the diamond cell window. Arrows indicate the changes with increasing pressure. The inserts show the pressure dependence of the spectral weight of the Drude contribution (solid squares), the 1000-cm^{-1} maximum (open squares), and the mid-infrared band (open circles).

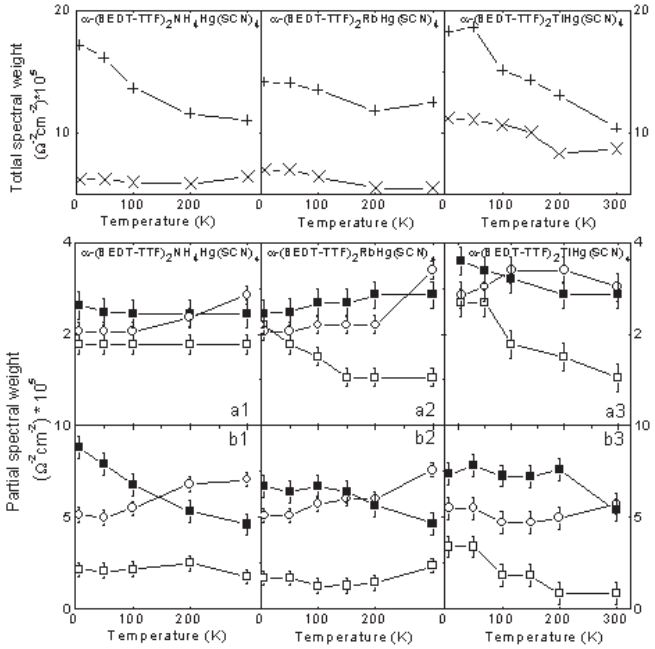

FIG. 5: Upper panel: temperature dependence of the total spectral weight for α-(BEDT-TTF)$_2M$Hg(SCN)$_4$ (M = NH$_4$, Rb, Tl) parallel to the stacks (diagonal crosses) and perpendicular to the stacks (straight crosses). Lower panel: Temperature dependence of the spectral weight for the three main features in the optical spectra of α-(BEDT-TTF)$_2M$Hg(SCN)$_4$ (M = NH$_4$, Rb, Tl) compounds: filled squares - Drude peak, empty squares - 1000 cm^{-1} maximum, empty circles - 2500 cm^{-1} maximum. (a) Polarization parallel to the stacks direction and (b) perpendicular to the stacks. Note different scales for the different contributions and polarizations.

phonons freeze out. (ii) The shrinking of the unit-cell volume increases the number of carriers proportionally. (iii) The transfer integrals and bandwidth become larger which reduces the V/t ratio.

The total spectral weight increases on cooling due to the thermal contraction of the unit cell volume (Fig. 5) and an increase of the bandwidth (See Sec. III B). However, in all cases the variation is more intense in the direction $E\perp$ stacks in agreement with the anisotropic temperature behavior calculated for the hopping integrals t.[31] The experimentally observed anisotropy is largest for the NH$_4$ compound, and decreases on going to Rb and Tl.

If no change of the ground state occurs, an increase of the transfer integrals in the $E\perp$ stacks direction on cooling will reduce the V/t ratio and lead to a redistribution of the spectral weight to the low-frequency features.[19] Although it is know that t changes as much as 10%, a quantitative prediction of the spectral weight shift turns out to be difficult; experimentally the assessment is easier. Indeed, in the conductivity spectra [$E \perp$ stacks, Figs. 1, 2, and 5(b)] of the NH$_4$ and Rb compounds the zero-frequency peak grows on the expense of the band around 2500 cm^{-1}; the tendency is more pronounced for the NH$_4$ salt. Interestingly, the redistribution of spectral weight does basically not involve the low-frequency maximum at 1000 cm^{-1}: the intensity of this feature is conserved. This strengthening of the metallic behavior leads to decrease of the effective mass upon cooling in the NH$_4$ and Rb spectra (Fig. 6). The Tl compound, however, shows a different tendency: the intensity of the maximum at 1000 cm^{-1} increases on cooling, which is suggestive for non-metallic behavior.

The same considerations suggest no redistribution of the spectral weight in the direction parallel to the stacks because the transfer integrals t do not increase upon thermal contraction, that is confirmed by the constant spectral weight for NH$_4$ and Rb compound in this direction.

F. In-plane anisotropy

One of the unusual features of the studied α-phase BEDT-TTF salts is the in-plane anisotropy. These compounds are considered to be quasi-two-dimensional conductors, and indeed, the in-plane conductivity has a metallic character in both directions. With optical means we can detect an in-plane anisotropy of approximately a factor of two: perpendicular to the stacks the conduc-

tivity is higher compared to the in-stack direction. This experimentally detected anisotropy in general agrees with the calculation of transfer integrals,[9] though the t-values are even more anisotropic.

The interesting point is the different temperature behavior for polarizations $E \parallel$ stacks and $E \perp$ stacks; again the latter one is 'more metallic'. This is in agreement with the anisotropy obtained in dc resistivity measurement for α-(BEDT-TTF)$_2$TlHg(SCN)$_4$:[37] while for $E\perp$ stacks resistivity is metallic, for the $E \parallel$ stacks it shows only a slow decrease with reduced temperature down to $200 - 150$ K, while for lower temperatures the slope becomes steeper.

Maesato *et al.*[38] investigated the resistivity for K and NH_4 compounds while applying uniaxial strain. They proposed that the anisotropy ρ_c/ρ_a defines the ground state of these salts, being larger for the NH_4 superconducting compound than for the K analog. These observations on in-plane anisotropy agree very well with our optical measurements which probe the transfer integrals in the plane: the optical anisotropy and the anisotropic temperature behavior of the spectral weight (see Fig. 5) is more pronounced for α-(BEDT-TTF)$_2$NH$_4$Hg(SCN)$_4$ compared to other members of the family.

IV. DISCUSSION: CHARGE ORDER FLUCTUATIONS *vs.* STATIC ORDER

A. Charge fluctuations effects

The NH_4 and Rb compounds show a striking decrease of effective mass m^*/m_b upon cooling (see Fig. 6), especially important is that this effect is seen for $E \parallel$ stacks polarization. While the strength of the effect in $E\perp$ stacks direction can be partly explained by the redistribution of the spectral weight to low frequencies due to thermal contraction of the crystal (see the above Section and Fig. 5), this is not the case for E$\parallel$stacks, where the effective Coulomb repulsion V/t does not change on cooling.[31] Nevertheless, lowering the temperature from 300 K down to 6 K leads to a reduction of the effective carrier mass by about 10% in the direction parallel to the stacks; the uncertainty in the data and analysis does not permit to give a functional dependence. Fig. 5 reveals that this effect is caused by the redistribution of the spectral weight from the mid-infrared to the zero-frequency peak, again pointing on a decrease of correlation effects.

The observed temperature dependence does not correspond to the behavior known from simple metals, for which only the scattering rate increases with temperature, whereas the concentration and mass of the carriers remain constant. On one hand, this tendency is opposite to the effects observed in the prime example of strongly correlated electron systems:[39,40] in heavy fermions the electronic interactions become more important towards low temperatures and consequently the effective mass is significantly enhanced by up to three orders of magnitude as $T \rightarrow 0$. On the other hand, exactly this behavior is predicted for strongly correlated two-dimensional quarter-filled metals close to the charge-order phase transition.[19,20] Theoretical investigations indicate that the critical ratio $(V/t)_c$, which separates the metal from the charge-ordered phase, shifts to the larger values, as depicted in Fig. 8. When cooling down vertically (constant V/t), we depart from the phase boundary and hence the system becomes more metallic leading to a decrease of the effective mass with temperature.[41] The observations for the NH_4 and Rb compounds are well interpreted as the retreat of these systems from the critical value of correlations $(V/t)_c$ that corresponds to a reduction of the effective carrier mass as calculated from the experimental Drude spectral weight.

The other parameter of the charge carriers, the scattering rate $1/\tau$, also shows a characteristic temperature behavior. As demonstrated in Fig. 6, for the NH_4 and Rb salts the scattering rate linearly changes with temperature down to a crossover temperature T^* at 50 K; below T^* the decrease becomes slower.

Charge fluctuations cause a linear temperature dependence $1/\tau(T) \propto T$ for $T > T^*$,[19,41] as commonly observed in the case of electrons interacting with boson-like excitation such as phonons. For $T < T^*$ the scattering rate increases quadratically, as expected from Fermi-liquid theory. Thus T^* identifies the temperature where charge-order fluctuations become important in the metallic state. In the phase diagram it defines the distance from the critical point at which the charge ordering transition occurs: $T^* \rightarrow 0$ as $V \rightarrow V_c$. The characteristic energy scale $k_B T^*$ is very small, $T^* \ll T_F$, when the system is sufficiently close to the charge-ordering transition. From the crossover temperature for NH_4, $T^* \approx 50$ K, the transfer integrals can be estimated to about be approximately 0.06 eV, which is in good agreement with band structure calculations of these compounds[9,42] and with the position of the electronic bands in the spectra.

The observed decrease of the effective mass on cooling and the linear dependence of the scattering rate on temperature demonstrate that these quarter-filled systems are close to charge order and show this particular behavior due to charge-order fluctuations, while also moving away from the phase border with charge order on cooling down.

A slope of the temperature dependence of the scattering rate is strikingly enhanced when going from the NH_4 to the Rb compound. Already in the raw data large differences in the scattering rate of the Drude-contribution are seen for the various α-(BEDT-TTF)$_2M$Hg(SCN)$_4$ salts: For the NH_4 compound the Drude-like peak becomes very narrow at low temperatures with an extremely small scattering rate, while for the Rb salt the zero-frequency contribution is much wider. Since these compounds are isostructural, the conduction mechanism should essentially be the same. One might argue that they contain different impurity and defect concentrations; however, this would lead to a temperature indepen-

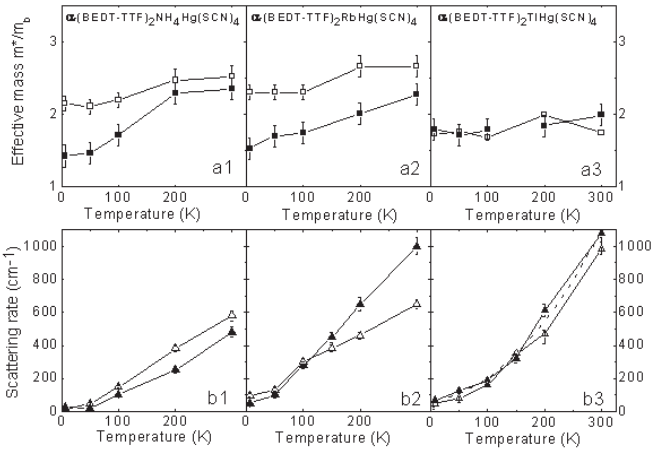

FIG. 6: Temperature dependence of the m^*/m_b (upper panel) and Drude-scattering rate γ (lower panel) for α-(BEDT-TTF)$_2M$Hg(SCN)$_4$ (M = NH_4, Rb, Tl) compounds: filled squares - $E\perp$ stacks, empty squares $E \parallel$ stacks. For the Tl-salt a $\gamma \sim T^2$ fit of the scattering rate is shown with a bold line.

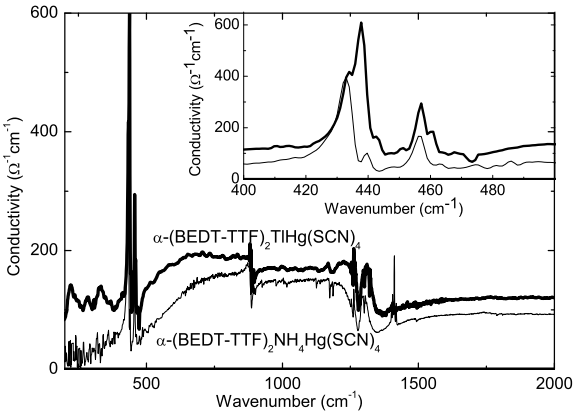

FIG. 7: The T=6 K spectra of α-(BEDT-TTF)$_2$TlHg(SCN)$_4$ (thick line) α-(BEDT-TTF)$_2$NH$_4$Hg(SCN)$_4$ (thin line) in E$\parallel$ stacks polarization. The insert shows the spectral range with $\nu_{12}(A_g)$ and $\nu_{13}(A_g)$ emv-coupled features for these two spectra. For α-(BEDT-TTF)$_2$TlHg(SCN)$_4$ to electronic band at 1000 cm^{-1} has higher intensity, and the vibrational features ar split, pointing on an ordered state.

dent offset in the scattering rate and cannot explain the distinct temperature dependence of the scattering rates observed for these compounds. We suggest, that the increase of the slope on going from NH_4 to Rb compound shows, the charge fluctuations are stronger in the latter one.[19]

Indeed, the values of the effective mass are also slightly higher for the Rb compound. In addition, the less metallic $E \parallel$ stacks polarization in the Rb salt shows a slight increase (up to 10% of intensity) of the 1000 cm^{-1} feature on cooling, also suggesting that the system is closer to the border with charge order.

B. Signatures of ordering in α-(BEDT-TTF)$_2$TlHg(SCN)$_4$

The most important tendency in the temperature behavior of the Tl compound is an increase of intensity of the 1000 cm^{-1} peak on cooling (see Fig. 5). This feature gets stronger at $T < 200$ K, while the Drude weight and the intensity of the high-frequency oscillator do not show such a big change.

Above we have assigned the peak around 1000 cm^{-1} to the short-range charge-order fluctuations, as suggested by exact diagonalization calculations .[19] Finding it in the spectra of all the compounds at room temperature infers that there is already some charge order present. However, it develops considerably when the Tl compound is cooled, while the effective mass in both polarization stays unchanged. This behavior evidences that in α-(BEDT-TTF)$_2$TlHg(SCN)$_4$ short-range charge order prevails although the compound does not become insulating. A similar behavior was found for α-(BEDT-TTF)$_2$KHg(SCN)$_4$ which remains metallic at any temperature, but shows strong indications of charge order in the optical spectra.[20]

We conclude that the decrease of the effective mass in the NH_4 and Rb compounds, on the one hand, and the increase of the 1000 cm^{-1} feature, on the hand, are competing processes: the two compounds are separated by a phase boundary or cross-over regime. Interestingly, for the direction parallel to the stacks the Rb compound shows a competing behavior below 100 K, inferring the presence of both effects; thus α-(BEDT-TTF)$_2$RbHg(SCN)$_4$ is located right on the boundary.

At the moment it is difficult to decide whether stable or fluctuating charge order dominates in α-(BEDT-TTF)$_2$TlHg(SCN)$_4$. From the temperature behavior of the scattering rate and vibrational features, we are inclined to assume the charge order to be more static. As indicated by a dashed line in Fig.6b3, the scattering rate has a temperature dependence close to a T^2-behavior in the entire temperature range. The origin of such a T^2 dependence in the full temperature range in contrast to the linear-T dependence of the other salts deserves further theoretical analysis and seems correlated to the observation of charge ordering phenomena

In addition to the optical response of the electronic system, we find some evidence of ordering in the vibrational features of the Tl compound. Due to the weak screening by the electronic background, the mode at about 400 cm^{-1} is clearly seen for the polarization $E \parallel$ stacks and allows detailed analysis. As Fig.7 shows, the $\nu_{12}(A_g)$ (based on D_2 symmetry) vibration shows up as a single band at 457 cm^{-1} for the NH_4 compound, while for α-(BEDT-TTF)$_2$TlHg(SCN)$_4$ the mode is split in two which are located at 457 and 460 cm^{-1}. The band of the

$\nu_{13}(A_g)$ vibration also splits: three bands at 433, 438, and 443 cm^{-1} (the latter one is very weak) can be distinguished for the Tl compound; for the NH_4 salt the band at 433 cm^{-1} is strong while only one weak peak is observed at 440 cm^{-1}. Some splitting also observed in the $\nu_6(A_g)$ anti-resonance feature in the spectrum of the Tl-salt. The Rb salt is again in the intermediate situation, showing a weak splitting of the $\nu_{13}(A_g)$. It should be noted, that the different splitting of the vibrational features is observed at temperatures below 200 K, being thus an evidence of a charge redistribution at the studied temperatures and is not connected to the low-temperature density wave state; however at higher temperatures the splitting could not be resolved due to higher bandwidth.

A closer inspection of the C-N stretching vibrations turns out to be helpful in our systems. According to the crystal structure, there are four SCN groups per unit cell; all of them are nearly parallel to the conducting layers and approximately perpendicular to the neighbors. Accordingly we observe up to four separate absorption bands of C-N vibrations. At $T = 6$ K when the bands are well resolved, the NH_4 and Rb compounds show two bands in each polarization; only the Tl salt shows all four C-N bands. This implies a lower symmetry or slightly different orientation of the SCN groups in the latter compound.

The lower symmetry of α-(BEDT-TTF)$_2$TlHg(SCN)$_4$ is in agreement with the above conclusion that this compound is closer to the charge-ordered state than the other salts and a static charge order is almost established.

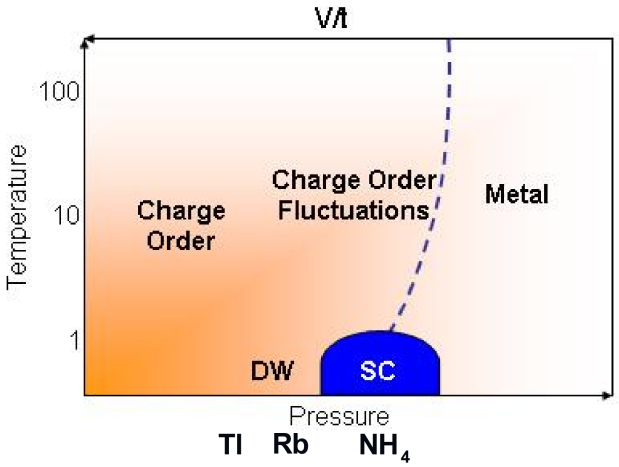

FIG. 8: Color online. Phase diagram for the quarter-filled two-dimensional organic conductors α-(BEDT-TTF)$_2M$Hg(SCN)$_4$ (M = NH_4, K, Rb, Tl). With increasing pressure the effective inter-site Coulomb repulsion V/t is reduced. At intermediate temperatures the system is tuned from a charge-order state (CO) to a metal with charge fluctuations in between. We propose that the compounds with M = K, Tl are to be found in this part of the phase diagram. We propose that the Rb-salt has lower influence of correlations, and the NH_4 salt is even less correlated, distinctly showing the increase of metallic properties on cooling, and becoming superconducting (SC) below 1 K.

V. CONCLUSIONS

Our optical studies on the quarter-filled α-(BEDT-TTF)$_2M$Hg(SCN)$_4$ (M=NH_4, Rb, Tl, K) evidence that in contrast to the half-filled compounds these two-dimensional conductors are metals with a Drude peak already developed at room temperature; but at the same time they show distinct spectral features caused by charge-order fluctuations. The spectral weight shift from the zero-frequency conductivity peak to higher frequencies leads to our assignment of electronic bands in the spectra. The findings of our optical measurements in the presence of external pressure confirm this interpretation. The features due to short-range charge order do not change on temperature for the NH_4 compound, whereas the effective mass of the charge carriers decreases on cooling. This observation agrees with the theoretically predicted re-entrance of the charge-order transition. Stronger electronic correlations in Tl salt increase the intensity of the spectral features due to charge order on cooling; the Rb compound shows the intermediate behavior. From the slope of the scattering rate and based on comparison to RPA predictions of a nearly charge ordered two-dimensional metals, we conclude that correlation effects intensify from NH4 to Rb. In contrast, Tl displays CO phenomena (as observed in the splitting of phonon modes) correlated with the presence of a different T behavior of scattering rate instead of the linear behavior of NH4 and Rb. This deserves further theoretical and experimental work. We suggest the order of these materials in a phase diagram in Fig. 8.

The presence of charge-order fluctuations is observed in all the studied salts but to a different degree. The less correlated is the NH_4 compound, which shows an increase of metallic properties on cooling, eventually becomes superconducting below $T_c = 1$ K. Thus we think that it is on the border (marked by a dashed line) between the charge order fluctuations and metallic state. On increasing the V/t ratio (moving to the left side of the phase diagram), this metallic behavior starts to compete with the charge order: the increase becomes obvious for the Rb salt. The Tl compound establishes short-range charge order upon cooling, and we would propose that it is the most correlated of the three studied materials. The same tendency with a strong increase of the respective spectral feature was observed in the K-salt.[20] This is in agreement with the observation of superconductivity under hydrostatic pressure in Ref.43

The temperature dependence of the scattering rate supports our conclusion that the influence of electronic correlations changes in this range of compounds.

Acknowledgments

We thank M. Calandra, M. Kartsovnik, M. Dumm, R.H. McKenzie, and H. Seo for helpful discussions. N.D. is grateful for the support of Alexander von Humboldt Foundation and to Russian President's grant "Leading Scientific schools" 5596.2006.2. The project was partially supported by the Deutsche Forschungsgemeinschaft (DFG), C.A.K. and A.P. acknowledge a support of Emmy-Noether-program. The crystal growth at Argonne was performed under the auspices of the Office of Basic Energy Sciences, Division of Material Sciences of the U.S. Department of Energy, Contract W-31-109-ENG-38.

* Present address: Experimentalphysik II, Universität Augsburg, D-86135 Augsburg, Germany

[1] N. D. Mathur, F. M. Grosche, S. R. Julian, I. R. Walker, D. M. Freye, R. K. W. Haselwimmer, and G. G. Lonzarich, Nature **394**, 39 (1998).

[2] G. Kotliar and D. Vollhardt, Physics Today, March 2004, p. 53.

[3] H. Seo, C. Hotta, and H. Fukuyama, Chem. Rev. **104**, 5005 (2004)

[4] R.H. McKenzie. *Science* **278**, 821 (1997).

[5] S. Lefebvre, P. Wzietek, S. Brown, C. Bourbonnais, D. Jerome, C. Meziere, M. Fourmigue, and P. Batail, Phys. Rev. Lett **85**, 5420 (2000).

[6] J. Merino and R. H. McKenzie, Phys. Rev. Lett. **87**, 237002 (2001).

[7] J. Wosnitza, *Fermi Surfaces in Low-Dimensional Organic Metals and Superconductors* (Spinger-Verlag, Berlin, 1996).

[8] J. Singleton, Rep. Prog. Phys. **63**, 1111 (2000).

[9] T. Mori, H. Inokuchi, H. Mori, S. Tanaka, M. Oshima, and G. Saito, J. Phys. Soc. Jpn, **59**, 2624 (1990).

[10] H. Mori, S. Tanaka, and T. Mori, Phys. Rev. B **57**, 12023 (1998).

[11] R.Chiba, K. Hiraki, T. Takahashi, H. M. Yamamoto, T. Nakamura, Phys. Rev. Lett. **93**, 216405 (2004).

[12] K. Suzuki, K. Yamamoto, M. Uruichi, and K. Yakushi, Synth. Met. **135-136**, 525 (2003).

[13] D. Schweitzer, P. Bele, H. Brunner, E. Gogu, U. Haeberlen, I. Hennig, I. Klutz, R. Swietlik, and H. J. Keller, Z. Phys. B , **67**, 489 (1987)

[14] M. Dressel, G. Grüner, J.P. Pouget, A. Breining, and D. Schweitzer, J. Phys. I (France) **4**, 579 (1994).

[15] S. Moroto, K.-I. Hiraki, Y. Takano, Y. Kubo, T. Takahashi, H. M. Yamamoto, and T. Nakamura. J. Phys. IV (France) **114** 339 (2004).

[16] M. Dressel and G. Grüner, *Electrodynamics of Solids* (Cambridge University Press, Cambridge, 2002).

[17] D. N. Basov , T. Timusk Rev. Mod. Phys. **77**, 721 (2005)

[18] M. Imada, A. Fujimori, and Y. Tokura Rev. Mod. Phys. **70**, 1039 (1998)

[19] J. Merino, A. Greco, R. McKenzie, and M. Calandra, Phys. Rev. B **68** 245121 (2003).

[20] M. Dressel, N. Drichko, J. Schlueter, and J. Merino, Phys. Rev. Lett. **90**, 167002 (2003).

[21] H. Mori, S. Tanaka, M. Oshima, G. Saito, T. Mori, Y. Maruyama, and H. Inokuchi, Bull. Chem. Soc. Jpn., **63**, 2183 (1990).

[22] C.C. Homes, M. Reedyk, D.A. Cradles, and T. Timusk, Applied Optics **32**, 2976 (1993).

[23] M. Dressel, J.E. Eldridge, H.H. Wang, U. Geiser, and J.M. Williams, Synth. Met. **52**, 201 (1992)

[24] H. Tajima, M. Inoue, R. Sakamoto, J. Yamazaki, and N. Hanasaki, Synth. Met. **133-134**, 151 (2003).

[25] H. K Mao, J. Xu, and P.M. Bell, J.Geophys. Res [Atmos.]**91**, 4673 (1986).

[26] C. A. Kuntscher, S. Frank, I. Loa, K. Syassen, T. Yamauchi, and Y. Ueda, Phys. Rev. B **71**, 220502(R) (2005).

[27] N. Drichko, M. Dressel, A. Kini, and J. Schlueter, Synth. Met. **133-134**, 91 (2003).

[28] K. Kornelsen, J.E. Eldridge, H.H. Wang, and J.M. Williams, Phys. Rev. B **44**, 5235 (1991).

[29] M. Dressel and N. Drichko, Chem. Rev. **104**, 5689 (2004).

[30] D. Faltermeier, J. Barz, M. Dumm, N. Drichko, M. Dressel, C. Meziere, and P. Batail, *to be published*; M. Dumm, D. Faltermeier, N. Drichko, M. Dressel, C. Meziere, P. Batail, J. Merino, and R. McKenzie, *to be published*

[31] S. Ono, T. Mori, S. Endo, N. Toyota, T. Sasaki, Y. Watanabe, and T. Fukase, Physica C **290**, 49 (1997).

[32] V. Vescoli, J.Favand, F. Mila, and L. Degiorgi. Eur. Phys. J. B **3** 149-154 (1998).

[33] N. Drichko and M. Dressel, to be published.

[34] S. Endo, W. Watanabe, T. Sasaki, T. Fukase, and N. Toyota. Synth. Met. **86**, 2013 (1997)

[35] H. Tajima, S. Kyoden, H. Mori, and S. Tanaka, Phys. Rev. B **62**, 9378 (2000).

[36] C. Campos, P. S. Sandhu, J. S. Brooks, T. Ziman, Phys. Rev. B **53**, 12725 (1996).

[37] A.I. Schegolev, V.N. Laukhin, A.G. Khomenko, M.V. Kartsovnik, R.P. Shibaeva, L.P. Rozenberg, and A.E. Kovalev, J. Phys. I (France) **2**, 2123 (1992).

[38] M. Maesato, Y. Kaga, R. Kondo, and S. Kagoshima. Phys. Rev. B **64** 155104 (2001)

[39] G.R. Stewart, Rev. Mod. Phys. **56**, 755 (1984).

[40] N. Grewe and F. Steglich, in: Handbook on the Physics and Chemistry of Rare Earths, Vol. **14**, ed. by K.A. Gscheidner Jr. and L. Eyring (Elsevier, Amsterdam, 1991), p. 343.

[41] J. Merino, A. Greco, N. Drichko, M. Dressel. Phys. Rev. Lett. **96**, 216402 (2006).

[42] H. Seo, C. Hotta, and H. Fukuyama, Chem. Rev. **104** (2004) 5005.

[43] D. Andres, M. V. Kartsovnik, W. Biberacher, K. Neumaier, E. Schuberth, and H. Müller. Phys. Rev. B, **72**, 174513 (2005).